

Article

Formulation of the Polymeric Double Networks (DNs) for Biomedical Applications with Physicochemical Properties to Resemble a Biological Tissue

Prutha Joshi ¹, Md Shakir Uddin Ahmed ², Komal Vig ² and Maria L. Auad ^{1,*}

¹ Department of Chemical Engineering, Center of Polymers and Advanced Composites, Auburn University, Auburn, AL 36849, USA; ppj0001@auburn.edu

² Department of Biological Sciences, Alabama State University, Montgomery, AL 36101, USA; mahmed@alasu.edu (M.S.U.A.); komalvig@alasu.edu (K.V.)

* Correspondence: auad@auburn.edu; Tel.: +1-3348445459

Abstract: Single-network hydrogels can have an internal porous structure and biocompatibility, but have lower mechanical properties. Combining these properties with another biocompatible and mechanically strong network can help in mimicking the extracellular matrix of native tissues to make them suitable for tissue scaffolds with desired performance. In the current objective, we combine the properties of poly (ethylene glycol) dimethacrylate (PEGDMA) macromer and polysaccharides as the two components in double networks (DN) for synergistic effects of both components resulting in the interpenetrating polymeric network for making it functional for replacement of injured tissues. The hydrogels were characterized by physical properties like swelling ratio, mechanical properties like tensile and compressive modulus, and rheological behavior. The chemical composition was studied using Fourier transform infrared spectroscopy (FTIR), and the thermal behavior using differential scanning calorimetry (DSC) experiments. Biodegradability and mechanical strength both are gained using double networks (DN), thus making it resemble more like living tissues. DN hydrogels were tested for cell compatibility for possible application in tissue engineering. Furthermore, these properties may allow their application as tissue-engineered scaffolds.

Keywords: double networks; polysaccharides; hydrogels; photopolymerization



Citation: Joshi, P.; Uddin Ahmed, M.S.; Vig, K.; Auad, M.L. Formulation of the Polymeric Double Networks (DNs) for Biomedical Applications with Physicochemical Properties to Resemble a Biological Tissue. *Sustain. Chem.* **2022**, *3*, 248–258. <https://doi.org/10.3390/suschem3020016>

Academic Editor: Li Chen

Received: 13 April 2022

Accepted: 23 May 2022

Published: 30 May 2022

Publisher's Note: MDPI stays neutral with regard to jurisdictional claims in published maps and institutional affiliations.



Copyright: © 2022 by the authors. Licensee MDPI, Basel, Switzerland. This article is an open access article distributed under the terms and conditions of the Creative Commons Attribution (CC BY) license (<https://creativecommons.org/licenses/by/4.0/>).

1. Introduction

Polymeric hydrogels are hydrophilic crosslinked networks that acquire an expanded three-dimensional structure when in a swollen state [1]. Although the physio-chemical properties of traditional hydrogels allow it to be valuable materials for biomedical applications like drug delivery [2–4], tissue engineering [5–7], molecular imprinting [3], and scaffolds [8–10], they lack biocompatibility. The rapid evolution of tissue engineering is accelerating the research for biodegradable and biocompatible materials to make them appropriate for the adhesion and proliferation of different types of cells [5,11]. Polysaccharides applications have been of particular interest among the synthetic and natural polymers that can be used for tissue engineering.

Most traditional hydrogels generally have low mechanical strength and elastic properties and possess biocompatibility issues, limiting their biomedical application scope [12]. In a hydrogel, mechanical strength is a property used to maintain its original shape. On the other hand, the biodegradability and biocompatibility can allow its adaptation to tissue movement and reformation [13]. However, these two properties can be contradictory [14] in the same hydrogels. Therefore, interpenetrating double networks are proposed to maintain the synergy between mechanical properties and biocompatibility and achieve the desired performance.

The double network hydrogels are interpenetrating or interlaced polymer networks at the molecular scale with different properties [15]. The properties of double network hydrogels prepared from two or more different polymer chains were reported to be much better than single polymer hydrogels [14,16,17]. Ordinary single network hydrogels, for example, poly (2-acrylamido-2-methylpropanesulfonic acid) (PAMPS) is said to have high hydrophilicity and good porosity. However, it has a compressive stress of only 0.4 MPa, which does not match the articular cartilage-like compressive strength (~36 MPa) as reported in the literature [12]. However, when a double network of poly(acrylamide) (PAAm) and PAMPS is produced, the authors indicate a 43 times higher compressive modulus than the PAMPS gel.

In particular, large numbers of hydrogel materials are from natural polysaccharides and proteins, such as gelatin, chitosan, hyaluronic acid, and many others. They have been rigorously researched for numerous biomedical applications due to their good biodegradability, biocompatibility, non-immunogenic performances, and abundant sources. Chitosan (polysaccharide), and gelatin (protein) have been widely used in the synthesis of hydrogels for tissue engineering due to their cell responsiveness and biocompatibility [18,19]. As reported by Li et al., the molecular chains of polysaccharides are very different, and as a consequence, the hydrogels are produced from them. Some are significantly stiffer and rigid, while others are flexible and elastic, developing various properties and potential applications. On the contrary, poly(ethylene glycol)-based hydrogels are biocompatible with outstanding elasticity, but their stiffness is low [14]. The three-dimensional porous structured double network hydrogel can be used to stimulate the combination of properties of both networks to mimic the cell-extracellular matrix. The excellent point to note is that the cartilage and other skeletal system tissues are high water-content materials and employ crosslinking with a double-network strategy (e.g., highly crosslinked collagen plus proteoglycan gel) to achieve their mechanical properties along with biocompatibility.

In Joshi et al., the poly (ethylene glycol) dimethacrylate (PEGDMA) hydrogels illustrated their biocompatibility and mechanical strength, along with the ability to grow and proliferate cells, to become viable for scaffolds in the tissue engineering field [20]. Moreover, PEGDMA was also used as a part of bio-ink formulation because of its mechanical and rheological performance for 3D printing using stereolithography [20]. Another research [19] reported that the polysaccharide-based hydrogels were prepared, and the range of properties corresponding to the kind of polysaccharide used in synthesis gives more flexibility to its application in tissue regeneration on designed hydrogel scaffolds.

In the current research, we focused on the synthesis of different double network hydrogels using poly (ethylene glycol) dimethacrylate, gelatin methacrylate, and chitosan methacrylate macromere as an interpenetrating polymer network. Hence, a UV-induced free radical polymerization was utilized to produce the double hydrogel networks. In addition, the physicochemical properties of the resulting samples were studied as well as fibroblast cell compatibility and growth.

2. Materials and Methods

For this research study, three varieties of linear poly (ethylene glycol) (PEG) were used: PEG (Mw~4000 g/mol) purchased from Bean Town Chemicals (BTC) (Hudson, NY, USA), PEG (Mw~6000 g/mol) and PEG (Mw~8000 g/mol), which were purchased from Acros Organics (Fair Lawn, NJ, USA). Gelatin powder (Type A, ~300 bloom) purchased from Electron Microscopy Sciences (Hatboro, PA, USA). Chitosan ($\geq 85\%$ deacetylated) was purchased from Alfa Aesar (Haverhill, MA, USA). Methacrylic anhydride was purchased from Thermofisher Scientific Inc. (Waltham, MA, USA). Dulbecco's phosphate buffered saline (DPBS) and acetic acid were purchased from VWR (Radnor, PA, USA). Photoinitiator, 1-hydroxycyclohexyl phenyl ketone (Irgacure 184) was purchased from TCI (Portland, OR, USA), while the UV light source used (UVLS-28 EL Series UV Lamp) was manufactured by Analytik Jena (Jena, Germany). Lysozyme purchased from Thermofisher Scientific Inc. (Waltham, MA, USA) was used for the degradation studies. Fibroblast cells were brought commercially (CCL 110; ATCC,

VA). Cells were cultured in DMEM (Gibco, Gaithersburg, MD, USA) supplemented with 10% *v/v* fetal bovine serum (Gibco, Gaithersburg, MD, USA). MTT (3-(4,5-Dimethylthiazol-2-yl)-2,5-Diphenyltetrazolium Bromide) salt was brought from Invitrogen (New York, NY, USA), and Live and Dead Double Staining Kit was bought from ThermoFisher Scientific Inc. (Waltham, MA, USA).

2.1. Preparation of Hydrogel Based on Double Networks (DN)

The individual polymeric systems (PEGDMA, GelMA, and ChMA) were first synthesized separately. Briefly, poly(ethylene glycol) (PEG) was mixed with 10 molar excess of methacrylic anhydride via microwave synthesis to obtain the PEGDMA samples [20]. Gelatin methacrylation was carried out using 5% (*w/v*) in Dulbecco's phosphate buffered saline (DPBS) and methacrylic anhydride (35.67 molar excess) at 60 °C [19]. It was then dialyzed for purification, followed by lyophilization at 0.12 mbar and −50 °C to obtain the pure gelatin methacrylate (GelMA) and stored at −80 °C until further use. Chitosan methacrylation was carried out using 3% (*w/v*) in 1–2% (*w/v*) acetic acid aqueous solution and methacrylic anhydride (35.67 molar excess) at 25 °C and was freeze-dried at 0.12 mbar and −50 °C to obtain the pure chitosan methacrylate (ChMA) and stored at −80 °C until further use [19].

The double network-based hydrogels were synthesized in two ways—(1) by dissolving 10% (*w/v*) of GelMA and 10% (*w/v*) of PEGDMA in DPBS buffer and (2) by dissolving 10% (*w/v*) ChMA and 10% (*w/v*) of PEGDMA in distilled water. Likewise, different PEGDMA-GelMA DN hydrogels were synthesized using three different PEGDMA samples with different molecular weights, 4000, 6000, and 8000 Da, as shown in Table 1. The degree of methacrylation calculated is listed in Table 1 in brackets or the polysaccharide hydrogels, as reported by Joshi et al. [19]. Irgacure 184 (2% *w/v*) was used as a photo-initiator for free-radical photopolymerization reaction (Figure 1).

Table 1. Nomenclature of Double Network hydrogels.

Double Network Hydrogels	PEGDMA 4000	PEGDMA 6000	PEGDMA 8000
GelMA (7%)	P4G7%	P6G7%	P8G7%
GelMA (16%)	P4G16%	P6G16%	P8G16%
GelMA (21%)	P4G21%	P6G21%	P8G21%
ChMA (40%)	NA	NA	P8C40%

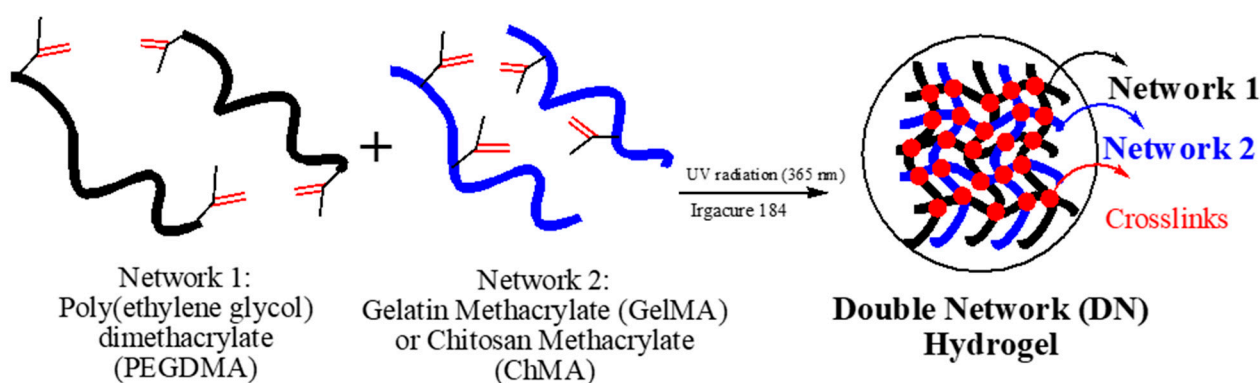


Figure 1. Photopolymerization reaction to obtain DN hydrogels.

The sample height during the UV curing was consistent in all the sample preparations. The UV lamp was kept just above the aluminum circular pans (recipient) with constant volume and duration of irradiation as 5–10 min. Synthesized hydrogels were rinsed with distilled water and stored in lyophilized conditions.

2.2. Characterization of Double Networks

The infrared spectra of the starting materials- PEGDMA powder, GelMA and ChMA, and final products- PEGDMA-GelMA DN and PEGDMA-ChMA DN hydrogel were measured by attenuated total reflection (ATR) method using a Thermo Nicolet 6700 Fourier transform infrared spectrometer. The spectrums were analyzed using OMNIC 7.3 software. All spectra were recorded between 400 and 4000 cm^{-1} over 256 scans with a resolution of 4 cm^{-1} .

The morphological structure of the hydrogels was investigated by scanning electron microscopy (SEM, Zeiss EVO 50 VP-SEM, Carl Zeiss Microscopy, LLC, White Plains, NY, USA) to obtain the topological characteristics of the hydrogels. After photo-crosslinking, swollen hydrogels were lyophilized in a freeze dryer. The fractured surfaces of pre-chilled hydrogels in liquid nitrogen were studied by SEM. The samples were mounted on aluminum support stubs with double-stick tape or fingernail polish. Then, the stubs were sputtered with gold (EMS Q150R sputter coating device) prior to SEM observations. The average pore size of the samples was quantified using ImageJ software.

Hydrogel samples were lyophilized in a freeze dryer and weighed to obtain dry sample weight (W_d). Then, samples were immersed in distilled water to swell at room temperature for about 48 h. The swollen hydrogels were removed from the water after wiping excess water on the surface and weighed to obtain a wet sample (W_w). Swelling ratios were calculated using the following equation:

$$\text{Mass Swelling (\%)} = \left(\frac{W_w - W_d}{W_d} \right) * 100 \quad (1)$$

Modulated differential scanning calorimetry (DSC) (modulate ± 0.531 $^{\circ}\text{C}$ every 60 s using a heating rate 5 $^{\circ}\text{C}/\text{min}$) was carried out to observe the change in crystallization temperature (T_c), melting temperature (T_m), and enthalpy of melting (ΔH_m) of the polymer networks. Polymer crystallinity can be determined with DSC by quantifying the heat associated with the melting (fusion) of the polymer. This heat is reported as percent crystallinity (% X_c) [21] by normalizing the observed heat of fusion (ΔH_m) to a 100% crystalline sample of the same polymer ($\Delta H_m^0 = 196.8$ J/g) [22]. The quantification of crystallinity is calculated from Equation (2), where $W_{\text{crystalline}}$ is the weight of the crystalline part in the double network hydrogel) in the PEGDMA based on reversible heat flow.

$$X_c (\%) = [\Delta H / (\Delta H_m^0 * W_{\text{crystalline}})] * 100 \quad (2)$$

The mechanical properties of the hydrogels were tested with the help of a dynamic mechanical analyzer (DMA) TA Instrument RSAIII. Compression testing analysis was carried out according to the ASTM D695-15 [23] on the specimens with 5 mm diameter and extension rate -0.067 mm/s at room temperature using the cylindrical compression geometry, performed for 3–6 replicates. From this data, the compression modulus was determined. Rheological measurements were obtained using a TA Instruments Rheology Advantage AR parallel plate rheometer fitted with 25 mm aluminum plate in the presence of air and at room temperature. Cylindrical samples (15 mm diameter and 1000 μm thickness) were cut and placed for strain sweep and frequency sweep experiments. From the strain sweep experiment performed at 1 Hz, 0.5% strain was selected (in the linear elastic range), which was then used as the constant strain in the oscillatory frequency sweep experiments. Tensile tests were performed according to the ASTM standards ASTM D1708-93 [24]. The tensile analysis was carried out on rectangular swollen hydrogels specimens with 15 mm initial length, using an extension rate of 0.1667 mm/s, for 3–6 replicates. During tensile testing, data for any hydrogel that slipped off the clamped area or broke as a result of being next to the metallic surface was not considered. From this data, the tensile modulus was determined.

The biodegradation analysis of double networks was performed in distilled water containing 600–900 mg/L of lysozyme [25,26] at 37 $^{\circ}\text{C}$. Enzymatic degradation was monitored

for four (4) weeks, while the enzyme solution was refreshed once. At a predetermined time (1, 2, 3, and 4 weeks), samples were removed from the medium and dried thoroughly. The weight of samples before (m_1) and after (m_2) the in vitro degradation was measured, and the degree of degradation (%) was determined relative to respective weight loss to the initial weight of the sample as follows:

$$\text{Degree of Degradation (\%)} = \left(\frac{m_1 - m_2}{m_1} \right) * 100 \quad (3)$$

2.3. Fibroblast Cell Attachment and Proliferation on the Hydrogel Scaffolds

Fibroblast cells were cultured in DMEM media with 10% FBS and 1% Penicillin-Streptomycin antibiotic solution at 37 °C in a 5% CO₂ incubator. The scaffolds were sterilized under UV for 30 min, followed by placement in a sterile plate with DMEM-10 media overnight. The following day fibroblast cells were seeded (50,000/well) on scaffolds. The scaffolds plated with cells were maintained in 5% CO₂ incubator at 37 °C. The cells were regularly monitored by using an optical microscope.

Cell viability of cells grown on scaffolds was measured by MTT (3-(4,5-dimethylthiazol-2-yl)-2,5-diphenyl-tetrazolium bromide) dye reduction. Fibroblast cells were seeded in a 96-well plate at a density of 20,000 cells per well in DMEM containing 10% FBS and grown overnight. At periodic time intervals, 10 µL of MTT (0.5 mg/mL) in sterile-filtered PBS was added to each well and incubated for 3 h to allow the formation of formazan crystals at 37 °C. DMSO (200 µL) was added to each well after incubation to dissolve the MTT formazan crystals and incubated for another 60 min at 37 °C. The absorbance of formazan products was measured at 570 nm using a microplate reader (Synergy LX, BioTek, Winooski, VT, USA). The percentage of live cell death was obtained by the difference between the absorbance of control cells and cells grown on scaffolds.

The seeding efficiency of fibroblast cells on hydrogels was investigated by plating 20,000 cells on the surface of each scaffold in a 48 well cell culture plate in 100 µL of media and incubated in 5% CO₂ incubator at 37 °C. After 30 min, an additional 200 µL of media was added and incubated. MTT assay was performed after 2 h of incubation to calculate the number of seeded cells. A 96-well without scaffold was plated with cells and was used as a control. Seeding efficiency was calculated using the following equation, where C is the absorbance of control cells and T is the absorbance of cells on the scaffold.

$$\text{Seeding efficiency (\%)} = \left(\frac{C - T}{C} \right) * 100 \quad (4)$$

3. Results and Discussion

3.1. Characterization of Double Networks

FTIR analysis of the PEGDMA-GelMA and PEGDMA-ChMA double networks after the free radical polymerization was performed, and the resulting FTIR spectra comparing the final networks with the original counterparts are displayed in Figure 2a,b.

In the GelMA spectrum (Figure 2a), particularly the peaks 1529 cm⁻¹ and the broader peak of 3321 cm⁻¹ correspond to N-H stretch of amide (II) [27–29]. The peaks visualized at 2938 and 1633 cm⁻¹ represent C-H stretch and C=O stretching vibrations in the GelMA spectrum [28]. The peaks corresponding to N-H and C=O are also seen in the spectrum of PEGDMA-GelMA DN, which gives evidence for the presence of GelMA polymer in the double network hydrogel. Similarly, the FTIR spectrum of ChMA (Figure 2b) depicts the peaks at 2930 and 1666 cm⁻¹ that visualize the C-H and C=O stretches of amide group, respectively [28,30]. Moreover, the 1055 cm⁻¹ peak belongs to C-O-C stretch and the 1543 cm⁻¹ represented N-H of amide (II) stretching mode [28] in ChMA spectrum. The peaks corresponding to N-H, C=O and C-O-C have also seen the spectrum of PEGDMA-ChMA DN, which gives evidence for the presence of ChMA polymer in the double network hydrogel. Additionally, PEGDMA marks its presence in both of these double networks as the strong bands at ~2880 cm⁻¹ and ~1466 cm⁻¹ represent C-H bonds [31,32] are present in

the spectra of PEGDMA as well as DNs. The bands at $\sim 1140\text{ cm}^{-1}$ and $\sim 960\text{ cm}^{-1}$ represent the asymmetrical C-O-C stretching mode [33] and are clearly observed in PEGDMA-GelMA, PEGDMA-ChMA, and PEGDMA spectra.

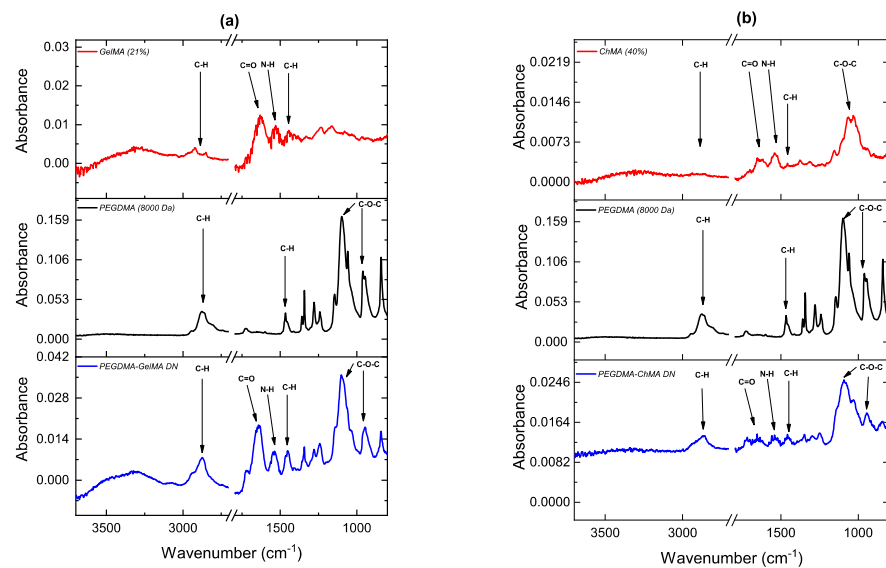


Figure 2. FT-IR spectrum for (a) GelMA (21%), PEGDMA (8000 Da) and PEGDMA-GelMA DN, (b) ChMA (40%), PEGDMA (8000 Da) and PEGDMA-ChMA DN.

Figure 3a–d shows the SEM micrograph of the freeze-dried DN hydrogels. These pictures reveal a well-defined 3D porous network of the hydrogel. The average pore sizes of PEGDMA 4000 Da, 6000 Da, 8000 Da, GelMA (21%) and ChMA (40%) are listed in Table 2 to compare single networks with the DN hydrogels. It shows pore size decreases, followed by an increase as we change the molecular weight of PEGDMA from 4000 Da to 8000 Da. The observed trend results from the effect of the molecular weight of PEGDMA. Please be noted that for the subsequent study, the degree of methacrylation for the GelMA was kept constant (21%), and consequently, the degree of crosslinking is constant for these networks.

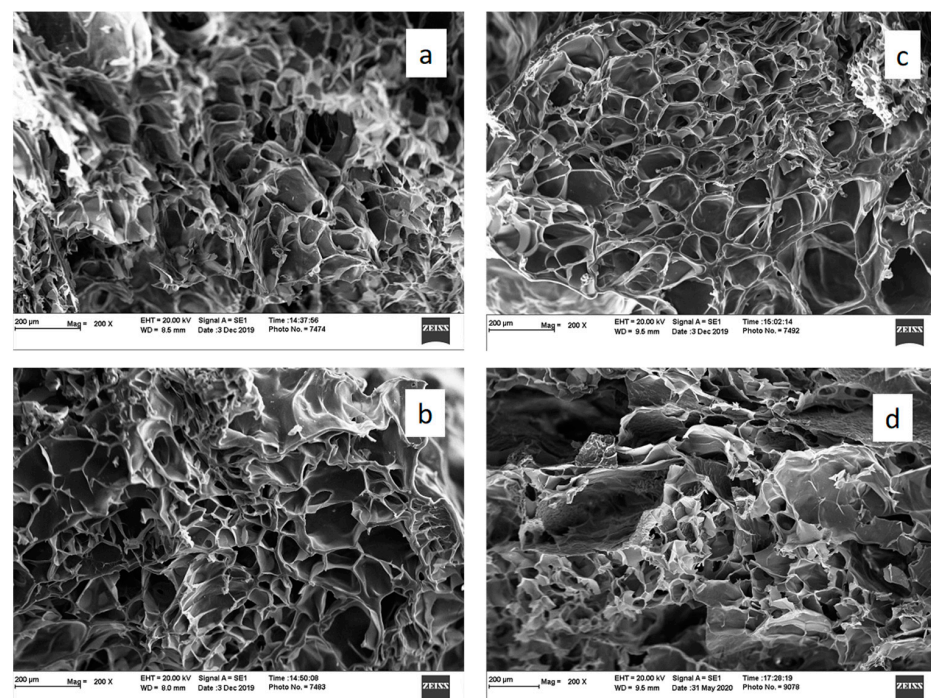


Figure 3. SEM image of (a) P4G21%, (b) P6G21%, (c) P8G21% and (d) P8C40% DN hydrogels.

Table 2. Comparison of morphology and swelling behavior for DN hydrogels.

	Pore Size (μm)	Swelling Ratio (%)
PEGDMA 4000	61.0 \pm 6.7	1400 \pm 230
PEGDMA 6000	72.0 \pm 12.7	1500 \pm 64
PEGDMA 8000	87.0 \pm 12.7	1900 \pm 140
GelMA (21%)	27.4 \pm 10.7	475 \pm 122
ChMA (40%)	68.1 \pm 14.4	2208 \pm 240
P4G21%	74.1 \pm 20.3	708 \pm 39
P6G21%	64.0 \pm 30.6	588 \pm 20
P8G21%	79.5 \pm 5.9	678 \pm 30
P8C40%	88.2 \pm 18.9	2033 \pm 463

The porous structure is crucial for the cell dwelling, proliferation, and cell culture on polymer-based hydrogel; on the other side, this open architecture affects the swelling and mechanical properties of the hydrogel, as can be observed in the following section.

The water uptakes (%) of the synthesized DN hydrogels were calculated using Equation (2). The obtained water uptake percentages are reported in Table 2 and show a decrease, followed by an increasing effect. The observed trend is the result of two effects, molecular weight of PEGDMA and degree of methacrylation of GelMA (21%) or ChMA (40%). As the molecular weight of PEGDMA is increased, the water uptake (or swelling ratio) should increase. However, in the case of the DN, the effect of the molecular weight between the PEGDMA produced crystallinity in the network, as can be observed in the subsequent sections.

Table 3 summarizes the heat of melting (ΔH_m) and melting temperatures (T_m) of the synthesized DN hydrogels. As the molecular weight of PEGDMA increases in the DN hydrogel, the crystallinity increases. Due to the increase in the molecular weight of PEG between crosslinking points, the linear PEG structure crystallized. As a result, the heat of melting increases, and the melting temperature elevates hence. This tendency is the result of the reduced segmental mobility of the network due to the crystalline phase. Similar results have also been reported in the literature [22].

Table 3. Characterization of the crosslinked DN hydrogels.

	T_m ($^{\circ}\text{C}$)	ΔH_m (J/g)	Crystallinity (%)	Compressive Modulus (kPa)	Shear Modulus (kPa)	Tensile Modulus (kPa)	Degradative Weight Loss (%)
P4G21%	22.83	17.93	18.2	8.41 \pm 1.1	3.67 \pm 0.05	8.4 \pm 2.3	39 \pm 1.6
P6G21%	29.57	25.37	25.8	10.8 \pm 2.3	6.42 \pm 0.86	13.9 \pm 2.6	34 \pm 1.2
P8G21%	44.23	27.79	28.2	9.97 \pm 1.2	4.04 \pm 0.85	16.1 \pm 3.7	32 \pm 1.1
P8C40%	27.33	7.15	7.3	77.6 \pm 11.0	13.8 \pm 1.1	21.2 \pm 6.7	37 \pm 1.3
GelMA (21%)	NA	NA	NA	30.4 \pm 7.2	4.0 \pm 0.6	NA	16 \pm 3.8
ChMA (40%)	NA	NA	NA	33.0 \pm 9.2	5.6 \pm 0.9	NA	35 \pm 5.5
PEGDMA 4000	48.42	70.57	35.9	17 \pm 7	2.7 \pm 0.73	13.1 \pm 6.5	23 \pm 1.1
PEGDMA 6000	56.31	109.3	55.5	18.8 \pm 6	4.31 \pm 0.68	20.7 \pm 6.1	24 \pm 1.2
PEGDMA 8000	57.93	151.6	77.0	16.5 \pm 4	1.9 \pm 0.43	31.3 \pm 9.7	28 \pm 1.4

In conclusion, the combined effect of crosslinking density and crystallinity affects the double network structure. As the molecular weight of the PEGDMA increases from 4000 Da to 8000 Da, the crystallinity increases. As a result, the porous structure and the water uptake (Table 2) show an opposite trend as expected. This effect will also be observed in the mechanical characterization of the networks.

The mechanical behavior of the hydrogels is reported in Table 3. It can be observed that the compressive and shear modulus show an increase followed by a decreased effect as the molecular weight of PEGDMA is increased. As we increase the molecular weight of PEGDMA, the molecular weight of the linear PEG increases the ability of the linear

chains to crystallize, thus increasing the modulus. However, at higher molecular weight, the decrease of the crosslinking densities overpowers the effect of the crystallinity, reducing the modulus.

Moreover, from Table 3, it can be concluded that the trend of tensile modulus of DN hydrogels is similar to what we observe in different PEGDMA networks. Hence, to conclude, the tensile property in DN hydrogels is governed by the PEGDMA network in the double network hydrogels.

Figure 4 shows the degradation behavior of synthesized DN hydrogels with degradative weight loss for a specific variety over a period of 8 weeks. In these experiments, a lysozyme solution served as the medium for biodegradation studies, which is similar to the physiological conditions found in the human body, which undergoes normal metabolism of degradation. As the exposure to the lysozyme enzyme solution increased, the degree of degradation was also increased. Figure 5 shows the morphology of DN hydrogels after 21 days of degradation. From the scanning electron microscopy (SEM), it is possible to observe the effect of the degradation process as the porous structure collapses and fibrillar structures are formed. It can be observed in Figure 5, the DN hydrogel with the higher crystallinity (P8G21%) degrades less compared to P4G21%. This trend is consistent with the expected results.

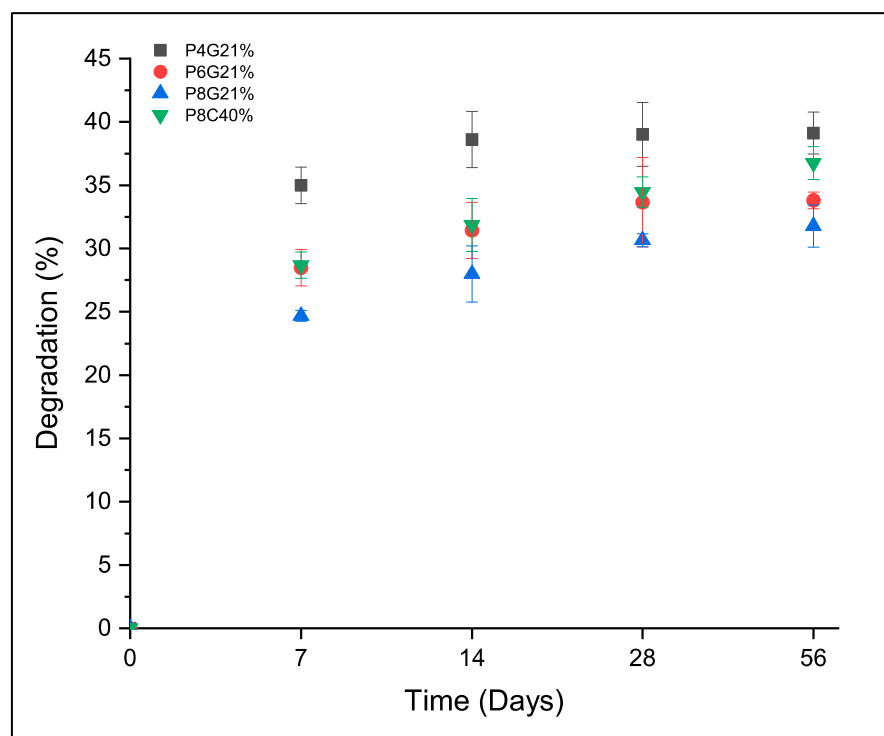


Figure 4. Degradation rate profile for different varieties of DN hydrogels with lysozyme.

3.2. Cell Growth and Proliferation on the Hydrogel Scaffolds

Seeding efficiencies for our designed scaffold P4G21%, P6G21%, P8G21% and P8C40% were 76.4%, 78.8%, 61.8% and 72.9%, respectively. To confirm cell attachment and viability, a live dead assay was utilized, and they were observed fluorescence. We observed fibroblast cell attachment and growth on the designed hydrogels for up to 7 days (Figure 6).

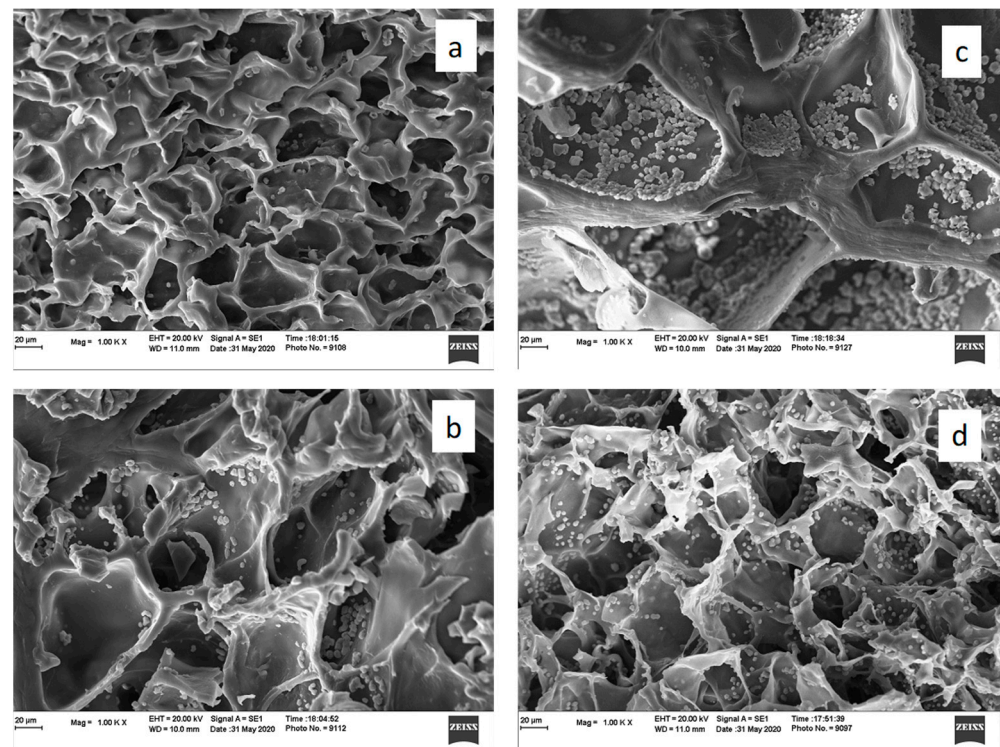


Figure 5. Effect on the morphology after 3 weeks of degradation of following DN hydrogels (a) P4G21%, (b) P6G21%, (c) P8G21%, and (d) P8C40%.

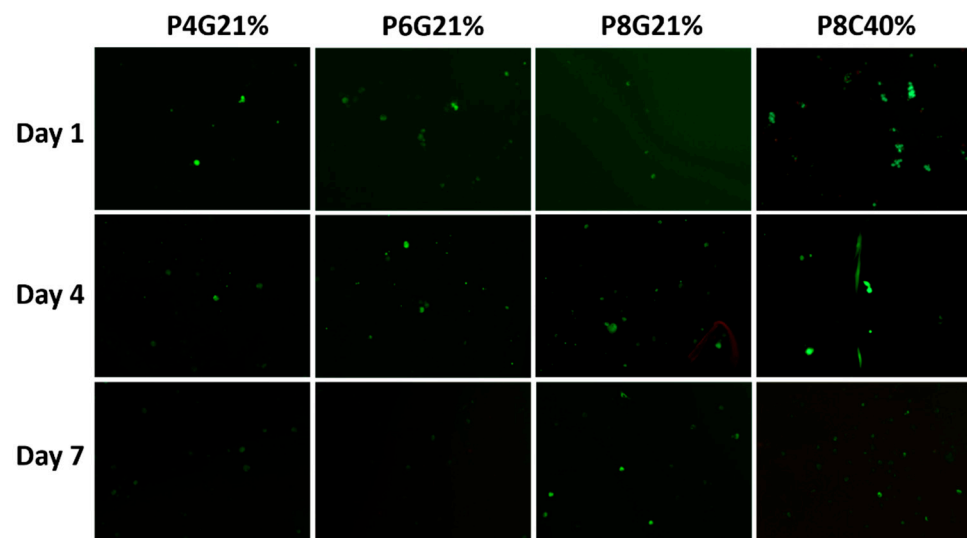


Figure 6. Fibroblast cell growth on DN hydrogels on P4G21%, P6G21%, P8G21%, and P8C40%. Live/Dead stain images of the cells.

Fibroblast cell viability was estimated using MTT assay and showed viable cells up to 7 days (Figure 7). We observed that all four formulations maintained Fibroblast cell growth. Cell viability on the designed scaffolds was 21–27% on Day 1 compared to cells grown without scaffold (control). By Day 7, cell viability was 25–30% on the designed scaffolds. Interestingly, among all the scaffolds, we observed increased cell viability up to 35.4% on P8C40% scaffold on Day 4 compared to 28.7%, 27.4%, and 26% on P4G21%, P6G21%, and P8G21%, respectively (Figure 7). However, the viability of cells decreased almost by 42–46% in 7 days on the designed scaffolds.

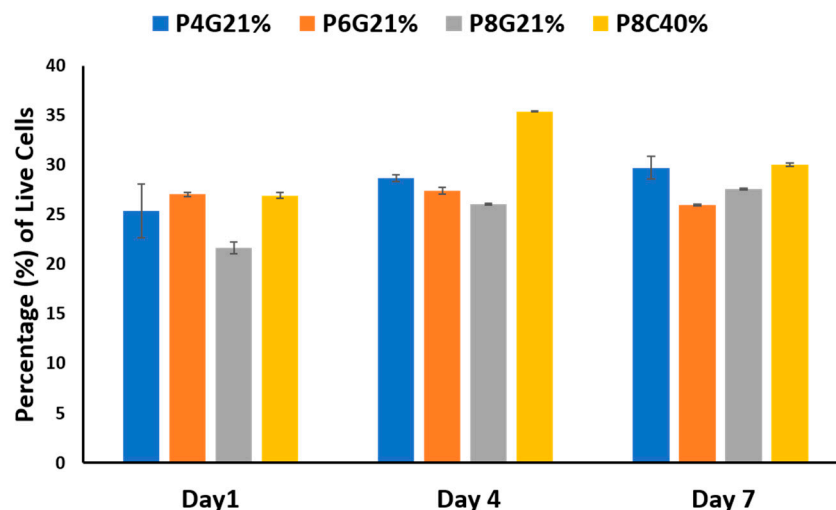


Figure 7. Cell viability of Fibroblast cells by MTT assay.

4. Conclusions

PEGDMA-GelMA and PEGDMA-ChMA double network hydrogels were synthesized using PEGDMA macromer of different molecular weights (4000 Da, 6000 Da, and 8000 Da) and modified polysaccharides such as GelMA and ChMA. Hydrogel samples undergo simultaneous free radical polymerization reaction in the presence of Irgacure 184 to obtain crosslinked double network (DN) hydrogels. The characterization of hydrogels illustrated their viability, biocompatibility, and mechanical strength for their applications in tissue engineering. Biodegradability and mechanical properties are obtained synergistically using double networks (DN), thus making it more like living tissues. Additionally, performed cell culture and proliferation studies in our research work suggest that double network hydrogels have the potential to become functional for tissue regeneration inside the human body.

Author Contributions: Conceptualization, M.L.A. and P.J.; methodology, P.J.; software, P.J.; validation, M.L.A., P.J. and K.V.; formal analysis, P.J.; investigation, P.J.; resources, K.V. and M.S.U.A.; data curation, P.J. and M.S.U.A.; writing—original draft preparation, P.J. and M.L.A.; writing—review and editing, P.J., M.L.A.; visualization, M.L.A.; supervision, M.L.A.; project administration, M.L.A.; funding acquisition, M.L.A. All authors have read and agreed to the published version of the manuscript.

Funding: This research was funded by NSF-CREST Center for Sustainable Lightweight Materials (C-SLAM), grant number #1735971.

Data Availability Statement: The data presented in this study are available on request from the corresponding author.

Conflicts of Interest: The authors declare no conflict of interest.

References

- Ahmed, E.M. Hydrogel: Preparation, characterization, and applications: A review. *J. Adv. Res.* **2015**, *6*, 105–121. [[CrossRef](#)] [[PubMed](#)]
- Kousar, F.; Malana, M.A.; Chughtai, A.H.; Khan, M.S. Synthesis and characterization of methacrylamide-acrylic acid-N-isopropylacrylamide polymeric hydrogel: Degradation kinetics and rheological studies. *Biomed. Mater.* **2018**, *155*, 1275–1298. [[CrossRef](#)]
- Caló, E.; Khutoryanskiy, V.V. Biomedical applications of hydrogels: A review of patents and commercial products. *Eur. Polym. J.* **2015**, *65*, 252–267. [[CrossRef](#)]
- Hoare, T.R.; Kohane, D.S. Hydrogels in drug delivery: Progress and challenges. *Polymer* **2008**, *49*, 1993–2007. [[CrossRef](#)]
- Fu, Y.; Xu, K.; Zheng, X.; Giacomini, A.J.; Mix, A.W.; Kao, W.J. 3D cell entrapment in crosslinked thiolated gelatin-poly (ethylene glycol) diacrylate hydrogels. *Biomaterials* **2012**, *33*, 48–58. [[CrossRef](#)] [[PubMed](#)]
- Gopinathan, J.; Noh, I. Recent trends in bioinks for 3D printing. *Biomater. Res.* **2018**, *22*, 11. [[CrossRef](#)]
- Khademhosseini, A.; Langer, R. Microengineered hydrogels for tissue engineering. *Biomaterials* **2007**, *28*, 5087–5092. [[CrossRef](#)]

8. Peppas, N.A.; Hilt, J.Z.; Khademhosseini, A.; Langer, R. Hydrogels in biology and medicine: From molecular principles to bionanotechnology. *Adv. Mater.* **2006**, *18*, 1345–1360. [[CrossRef](#)]
9. Baolin, G.; Ma, P.X. Synthetic biodegradable functional polymers for tissue engineering: A brief review. *Sci. China Chem.* **2014**, *57*, 490–500.
10. Cheng, Y.; Lu, J.; Liu, S.; Zhao, P.; Lu, G.; Chen, J. The preparation, characterization and evaluation of regenerated cellulose/collagen composite hydrogel films. *Carbohydr. Polym.* **2014**, *107*, 57–64. [[CrossRef](#)]
11. Matricardi, P.; Di Meo, C.; Coviello, T.; Hennink, W.E.; Alhaique, F. Interpenetrating polymer networks polysaccharide hydrogels for drug delivery and tissue engineering. *Adv. Drug Deliv. Rev.* **2013**, *65*, 1172–1187. [[CrossRef](#)] [[PubMed](#)]
12. Arnold, M.P.; Daniels, A.U.; Ronken, S.; Ardura García, H.; Friederich, N.F.; Kurokawa, T.; Gong, J.P.; Wirz, D. Acrylamide Polymer Double-Network Hydrogels: Candidate Cartilage Repair Materials with Cartilage-Like Dynamic Stiffness and Attractive Surgery-Related Attachment Mechanics. *Cartilage* **2011**, *2*, 374–383. [[CrossRef](#)] [[PubMed](#)]
13. Li, H.; Wang, H.; Zhang, D.; Xu, Z.; Liu, W. A highly tough and stiff supramolecular polymer double network hydrogel. *Polymer* **2018**, *153*, 193–200. [[CrossRef](#)]
14. Li, Z.; Wu, C.; Liu, Z.; Li, Z.; Peng, X.; Huang, J.; Ren, J.; Wang, P. A polypropylene mesh coated with interpenetrating double network hydrogel for local drug delivery in temporary closure of open abdomen. *RSC Adv.* **2020**, *10*, 1331–1340. [[CrossRef](#)]
15. Haque, M.A.; Kurokawa, T.; Gong, J.P. Super tough double network hydrogels and their application as biomaterials. *Polymer* **2012**, *53*, 1805–1822. [[CrossRef](#)]
16. Lei, K.; Li, Z.; Zhu, D.; Sun, C.; Sun, Y.; Yang, C.; Zheng, Z.; Wang, X. Polysaccharide-based recoverable double-network hydrogel with high strength and self-healing properties. *J. Mater. Chem. B* **2020**, *8*, 794–802. [[CrossRef](#)] [[PubMed](#)]
17. Monteiro, N.; Thirvikraman, G.; Athirasala, A.; Tahayeri, A.; França, C.M.; Ferracane, J.L.; Bertassoni, L.E. Photopolymerization of cell-laden gelatin methacryloyl hydrogels using a dental curing light for regenerative dentistry. *Dent. Mater.* **2018**, *34*, 389–399. [[CrossRef](#)]
18. Joshi, P.; Ahmed, M.S.U.; Vig, K.; Vega Erramuspe, I.B.; Auad, M.L. Synthesis and characterization of chemically crosslinked gelatin and chitosan to produce hydrogels for biomedical applications. *Polym. Adv. Technol.* **2021**, *32*, 2229–2239. [[CrossRef](#)]
19. Joshi, P.; Breaux, S.; Naro, J.; Al, E. Synthesis and characterization of photopolymerizable hydrogels based on poly (ethylene glycol) for biomedical applications. *J. Appl. Polym. Sci.* **2021**, *138*, e50489. [[CrossRef](#)]
20. Blaine, R.L. *Determination of Polymer Crystallinity by DSC*; TA Instruments: New Castle, DE, USA, 2010; pp. 1–3.
21. Pielichowski, K.; Flejtuch, K. Differential Scanning Calorimetry Studies on Poly (ethylene Glycol) with Different Molecular Weights for Thermal Energy Storage Materials. *Polym. Adv. Technol.* **2002**, *13*, 690–696. [[CrossRef](#)]
22. *ASTMD695-15*; Standard Test Method for Compressive Properties of Rigid Plastics. Astm International: West Conshohocken, PE, USA, 2015.
23. *ASTMD1708-93*; Standard Test Method for Tensile Properties of Plastics by Use of Microtensile Specimens. Astm International: West Conshohocken, PE, USA, 1993.
24. Lončarević, A.; Ivanković, M.; Rogina, A. Lysozyme-Induced Degradation of Chitosan: The Characterisation of Degraded Chitosan Scaffolds. *J. Tissue Repair Regen.* **2017**, *19*, 177. Available online: www.openaccesspub.org (accessed on 15 November 2019). [[CrossRef](#)]
25. Thakur, V.K.; Thakur, M.K. (Eds.) *Handbook of Polymers for Pharmaceutical Technologies, Biodegradable Polymers*; Scrivener Publishing: Beverly, MA, USA, 2015.
26. Sarem, M.; Moztafzadeh, F.; Mozafari, M.; Shastri, V.P. Optimization strategies on the structural modeling of gelatin/chitosan scaffolds to mimic human meniscus tissue. *Mater. Sci Eng. C.* **2013**, *33*, 4777–4785. [[CrossRef](#)] [[PubMed](#)]
27. Saraiva, S.M.; Miguel, S.P.; Ribeiro, M.P.; Coutinho, P.; Correia, I.J. Synthesis and characterization of a photocrosslinkable chitosan-gelatin hydrogel aimed for tissue regeneration. *RSC Adv.* **2015**, *5*, 63478–63488. [[CrossRef](#)]
28. Yang, C.; Xu, L.; Zhou, Y.; Zhang, X.; Huang, X.; Wang, M.; Han, Y.K.; Zhai, M.; Wei, S.L.J. A green fabrication approach of gelatin/CM-chitosan hybrid hydrogel for wound healing. *Carbohydr. Polym.* **2010**, *82*, 1297–1305. [[CrossRef](#)]
29. Monier, M.; Wei, Y.; Sarhan, A.A.; Ayad, D.M. No Title. *Polymer* **2010**, *51*, 1002–1009. [[CrossRef](#)]
30. Escudero-Castellanos, A.; Ocampo-García, B.E.; Domínguez-García, M.V.; Flores-Estrada, J.; Flores-Merino, M.V. Hydrogels based on poly (ethylene glycol) as scaffolds for tissue engineering application: Biocompatibility assessment and effect of the sterilization process. *J. Mater. Sci Mater. Med.* **2016**, *27*, 176. [[CrossRef](#)]
31. Guo, X.; Wang, W.; Wu, G.; Zhang, J.; Mao, C.; Deng, Y.; Xia, H. Controlled synthesis of hydroxyapatite crystals templated by novel surfactants and their enhanced bioactivity. *New J. Chem.* **2011**, *35*, 663–671. [[CrossRef](#)]
32. Cheing, B.W.; Ibrahim, N.A.; Yunus, W.M.Z.W.; Hussein, M.Z. Poly (lactic acid)/poly (ethylene glycol) polymer nanocomposites: Effects of graphene nanoplatelets. *Polymers* **2013**, *6*, 93–104. [[CrossRef](#)]
33. Yasmin, M.; Gupta, M. Thermodynamical Study of Alcoholic Solutions of Poly (ethylene glycol) Diacrylate and Poly (ethylene glycol) Dimethacrylate. *Int. J. Thermodyn.* **2012**, *15*, 111–117. [[CrossRef](#)]